Check for updates

Received: 11 September 2023 | Revised: 5 May 2024 | Accepted: 23 May 2024

DOI: 10.1111/apha.14186

ACTA PHYSIOLOGICA

RESEARCH PAPER

ATP6V1A is required for synaptic rearrangements and plasticity in murine hippocampal neurons

Alessandro Esposito[1] | **Sara Pepe**[1,2] | **Maria Sabina Cerullo**[3] | **Katia Cortese**[1] | **Hanako Tsushima Semini**[1] | **Silvia Giovedì**[1,2] | **Renzo Guerrini**[4,5] | **Fabio Benfenati**[2,3] | **Antonio Falace**[4,6] | **Anna Fassio**[1,2]

[1]Department of Experimental Medicine, University of Genoa, Genoa, Italy

[2]IRCCS, Ospedale Policlinico San Martino, Genoa, Italy

[3]Center for Synaptic Neuroscience and Technology, Italian Institute of Technology, Genoa, Italy

[4]Children's Hospital A. Meyer IRCCS, Florence, Italy

[5]Dipartimento di Neuroscienze, Psicologia, Area del Farmaco e Salute del Bambino, University of Florence, Florence, Italy

[6]Pediatric Neurology and Muscular Diseases Unit, IRCCS Istituto "Giannina Gaslini", Genoa, Italy

Correspondence
Anna Fassio, Department of Experimental Medicine, University of Genoa, Viale Benedetto XV, Genova 3 16122, Italy.
Email: afassio@unige.it

Present address
Alessandro Esposito, Division of Neuroscience, IRCCS San Raffaele Scientific Institute, Milan, Italy

Maria Sabina Cerullo, Department of Brain Sciences, Imperial College London, London, UK

Funding information
#NEXTGENERATIONEU (NGEU) and funded by the Ministry of University and Research (MUR), National Recovery and Resilience Plan (NRRP), project MNESYS (PE0000006)—A multiscale inte- grated approach to the study of the nervous system in health and disease (DN. 1553 11.10.2022).; The Italian Ministry of Health (Ricerca Finalizzata Giovani Ricercatori GR-2019-12 370 176); IRCCS Ospedale Policlinico San Martino (5x1000 and Ricerca Corrente); Tuscany Region Call for Health 2018 (grant DECODE-EE); Fondazione Cassa di Risparmio di Firenze (Human Brain Optical Mapping Project); University of Genoa (Grant D.R. 3404, Heavy Equipment)

Abstract

Aim: Understanding the physiological role of ATP6V1A, a component of the cytosolic V_1 domain of the proton pump vacuolar ATPase, in regulating neuronal development and function.

Methods: Modeling loss of function of *Atp6v1a* in primary murine hippocampal neurons and studying neuronal morphology and function by immunoimaging, electrophysiological recordings and electron microscopy.

Results: *Atp6v1a* depletion affects neurite elongation, stabilization, and function of excitatory synapses and prevents synaptic rearrangement upon induction of plasticity. These phenotypes are due to an overall decreased expression of the V_1 subunits, that leads to impairment of lysosomal pH-regulation and autophagy progression with accumulation of aberrant lysosomes at neuronal soma and of enlarged vacuoles at synaptic boutons.

Conclusions: These data suggest a physiological role of ATP6V1A in the surveillance of synaptic integrity and plasticity and highlight the pathophysiological

Alessandro Esposito and Sara Pepe equally contributed to this study.

This is an open access article under the terms of the Creative Commons Attribution-NonCommercial-NoDerivs License, which permits use and distribution in any medium, provided the original work is properly cited, the use is non-commercial and no modifications or adaptations are made.
© 2024 The Author(s). *Acta Physiologica* published by John Wiley & Sons Ltd on behalf of Scandinavian Physiological Society.

significance of ATP6V1A loss in the alteration of synaptic function that is associated with neurodevelopmental and neurodegenerative diseases. The data further support the pivotal involvement of lysosomal function and autophagy flux in maintaining proper synaptic connectivity and adaptive neuronal properties.

KEYWORDS

ATP6V1A, autophagy, LTP, lysosome, neurodevelopment, synapse, v-ATPase

1 | INTRODUCTION

Vesicular or vacuolar-type adenosine triphosphatase (v-ATPase) is a highly conserved multimeric complex that drives the transport of hydrogen ions upon ATP hydrolysis. In mammals, the complex is composed of the V_0 membrane domain, which consists of 7 distinct subunits and forms the hydrogen pore, and the V_1 cytosolic domain, which consists of 8 distinct subunits that bind and hydrolyze ATP.[1] The association/dissociation of V_0 and V_1 is reversible and regulates the proton pumping activity. Its activity is modified by several signals, including nutrients, hydrogen ion concentration, growth factors and kinases.[2–4] v-ATPase is embedded in various cellular membranes and the various subunits are typically expressed in a tissue-specific manner, resulting in different degrees of regulated acidification.[5,6] At lysosomal compartments, v-ATPase mediates the luminal acidification necessary for catabolic processes, such as endocytic degradation and autophagy. Autophagy is particularly relevant for neuronal cells, due to their post-mitotic nature, polarized morphology and high protein load, which sustain synaptic activity and plasticity.[7] In neurons, v-ATPase is additionally expressed by synaptic vesicles (SVs), where it creates the proton gradient that drives the loading of neurotransmitters.[8,9] Mutations in genes encoding the different subunits of v-ATPase and their regulators have been recently described in patients with a spectrum of neurodevelopmental disorders often associated with mental retardation and seizures.[10–18] In addition, loss of expression of ATP6V1A has been reported for late onset Alzheimer disease (AD).[19–21]

The atomic structure of the mammalian brain v-ATPase has been recently resolved, showing that the ATP6AP1 and ATP6AP2 subunits act as assembly factors for the V_0 domain.[22] Specific functions of the neuronal v-ATPase subunits have been investigated. However, due to the complexity of the supramolecular complex, a complete picture of their roles in the neuronal system is far from being elucidated. For instance, both the membrane-associated ATP6V0A1 subunit and the V_0 assembly factor ATP6AP2 have been shown to play a role in brain development in terms of synaptic integrity and connectivity.[10,17] Moreover, experimental evidence supports a complex and not fully elucidated role of the different members of the v-ATPase at presynaptic sites. The V_0 domain subunits V_0a and V_0c interact with the SNARE complex and modulate neurosecretion,[23,24] whereby V_1/V_0 disassembly represents a precondition for SV fusion, thus defining availability of SV for release.[25] Assembled V_1/V_0 was also identified on clathrin-coated endocytosed vesicles, where clathrin blocks v-ATPase activity and prevents acidification before uncoating.[26]

In accordance with the above-mentioned essential roles of v-ATPase, alterations in genes encoding v-ATPase subunits or their regulators were found to perturb brain development and synaptic function in animal models and cause human disease.[10–18]

v-ATPase dysfunctions were also described in aging and neurodegeneration.[27] In particular, deficits in *ATP6V1A* – encoding for the ubiquitously expressed subunit A of the V_1 complex – have been associated with both early-onset epileptic encephalopathy (EOEE)[14,16] and late onset AD.[19–21] These findings reveal that early neurodevelopmental and neurodegenerative disorders may share common pathways such as lysosomal and autophagic failures as consequence of neuronal v-ATPase dysfunction.

To investigate the role of v-ATPase in neuronal development and connectivity, we developed an in vitro neuronal model of*Atp6v1a* loss. We demonstrated that Atp6v1a depletion results in overall decrease of V_1 subunits, affects synapse stabilization and prevents long-term potentiation (LTP) at excitatory hippocampal synapses. These phenotypes were due to impairment of neuronal pH homeostasis and of autophagy with the accumulation of aberrant lysosomes at neuronal cell bodies and enlarged cisternae at synapses.

2 | RESULTS

2.1 | Loss of *Atp6v1a* impairs neuronal lysosomal acidification

We modeled neuronal *Atp6v1a* loss by silencing its expression in cultured primary rat neurons using RNAi-mediated knockdown. A small hairpin (sh)-RNA, targeting the coding sequence of the rat *Atp6v1a* mRNA (*Atp6v1a* KD), was generated and cloned into lentiviral vector for neuronal infection. Neurons were transduced at 10 days in vitro

17481716, 2024, 8, Downloaded from https://onlinelibrary.wiley.com/doi/10.1111/apha.14186 by Universita Di Firenze Sistema, Wiley Online Library on [04/08/2026]. See the Terms and Conditions (https://onlinelibrary.wiley.com/terms-and-conditions) on Wiley Online Library for rules of use; OA articles are governed by the applicable Creative Commons License

(DIV) and analyzed at 17 DIV. Western blot analysis revealed a significant reduction of Atp6v1a protein in *Atp6v1a* KD with respect to control neurons transduced with the scrambled sh-RNA virus (Figure 1A). By evaluating the expression of other v-ATPase subunits, we observed a parallel reduction of different members of the V_1 domain – namely Atp6v1h, Atp6v1b2 and Atp6v1c1- with no change in the V_0 subunit Atp6v0a1 (Figure 1A).

Loss of expression and activity of v-ATPase subunits in neurons is predicted to primarily impair intracellular pH homeostasis.[28,29] We therefore analyzed the consequences of Atp6v1a depletion on intraorganellar acidification, using the acidic dye Lysotracker (LTR). Staining with LTR was significantly lower in *Atp6v1a* silenced neurons, and the decrease in the LTR intensity was phenocopied in neurons treated with the v-ATPase blocker bafilomycin (Figure 1B,C). To verify the specificity of the phenotype and exclude off-target effects, we designed an ATP6V1A expressing construct that is resistant to silencing (r-ATP6V1A). Its efficacy was tested by western blot and immunocytochemistry (Figure S1). Re-expression of r-ATP6V1A in *Atp6v1a* KD neurons restored LTR intensity to control levels while no significant impact was observed in control scamble-sh-RNA transduced cells (Figure 1D).

These data demonstrate that the observed LTR phenotype is specifically associated to Atp6v1a loss and caused by inhibition of v-ATPase activity due to overall decrease of V1 subunits.

2.2 | The acidic shift in *Atp6v1a* KD neurons primarily involves lysosomes

To determine if the LTR decrease was cell autonomous and mainly affected lysosomal structures, we transfected neurons with *Atp6v1a* sh-RNA alone or together with the red fluorescent protein (RFP)-tagged lysosomal marker LAMP1 (LAMP1-RFP). LTR signal was heavily reduced in transfected cells (Figure 2A) and significantly lower in the LAMP1-positive compartments of both *Atp6v1a* KD transfected and bafilomycin-treated neurons (Figure 2B,C). These data suggest that the effect of *Atp6v1a* KD is cell autonomous and the basic shift at neuronal soma primarily involves lysosomes.

2.3 | *Atp6v1a*-silencing in neurons induces blockade of autophagy and lysosome ultra-structural alterations

v-ATPase-mediated acidification is necessary for lysosomal function and autophagic progression. To analyze the effects of *Atp6v1a* silencing on neuronal autophagy, we evaluated the expression of autophagic markers and revealed an accumulation of LC3 and p62 in the soma of neurons transduced with *Atp6v1a* KD with respect to that with scramble controls (Figure 3A,B). When analyzed by Western blot, we confirmed an increased expression of the autophagic markers Lc3 and p62 and revealed a net accumulation of Lc3-II, the lipidated form of Lc3 (Figure 3C). The phenotype was phenocopied by *Atp6v1a*-sh-RNA transfection and bafilomycin treatment (Figure S2). These data support the pivotal role of ATP6V1A expression and v-ATPase activity in sustaining autophagy progression in neurons.

When analyzed at the ultrastructural level, *Atp6v1a*-silenced neurons displayed increased density and size of multilamellar bodies (MLBs) in the soma, reminiscent of terminal non-degradative lysosomes (Figure 3D). Taken together these findings demonstrate that knockdown of the *Atp6v1a* subunit results in a prominent lysosomal alteration associated with impaired autophagy.

2.4 | *Atp6v1a* silencing impairs dendritic outgrowth and synaptogenesis due to selective loss of presynaptic sites

To examine the impact of the Atp6v1a loss on neuronal morphology and function, we quantified neurite arborization and synaptic connections in *Atp6v1a*-silenced neurons. Sparse transfected neurons, showed a significant decrease in neurite complexity, quantified by Sholl analysis (Figure 4A). The phenotype is accompanied by a significant loss of excitatory synaptic contacts, identified by the presynaptic marker v-Glut1 and the postsynaptic marker Homer 1. When analyzed separately, a significant decrease was observed only for the presynaptic transporter, suggesting a primary role of Atp6v1a at presynaptic sites (Figure 4B). Such decrease was phenocopied treating neurons with bafilomycin, implying that loss v-ATPase activity results in defective neuronal development and synaptic connectivity (Figure S3).

Single cell re-expression of r-ATP6V1A, in neuronal network silenced by viral transduction, efficiently restored the density of v-Glut1 positive puncta to the control level (Figure 4C).

These data demonstrate a specific impairment of neurite development and excitatory synaptic contact upon loss of V_1 subunits and v-ATPase dysfunction.

2.5 | Loss of Atp6v1a decreases the frequency of miniature excitatory postsynaptic currents and results in cisternae accumulation at presynaptic sites

To directly measure glutamatergic neurotransmission, we performed whole-cell voltage-clamp recordings of

17481716, 2024, 8, Downloaded from https://onlinelibrary.wiley.com/doi/10.1111/apha.14186 by Universita Di Firenze Sistema, Wiley Online Library on [04/08/2026]. See the Terms and Conditions (https://onlinelibrary.wiley.com/terms-and-conditions) on Wiley Online Library for rules of use; OA articles are governed by the applicable Creative Commons License

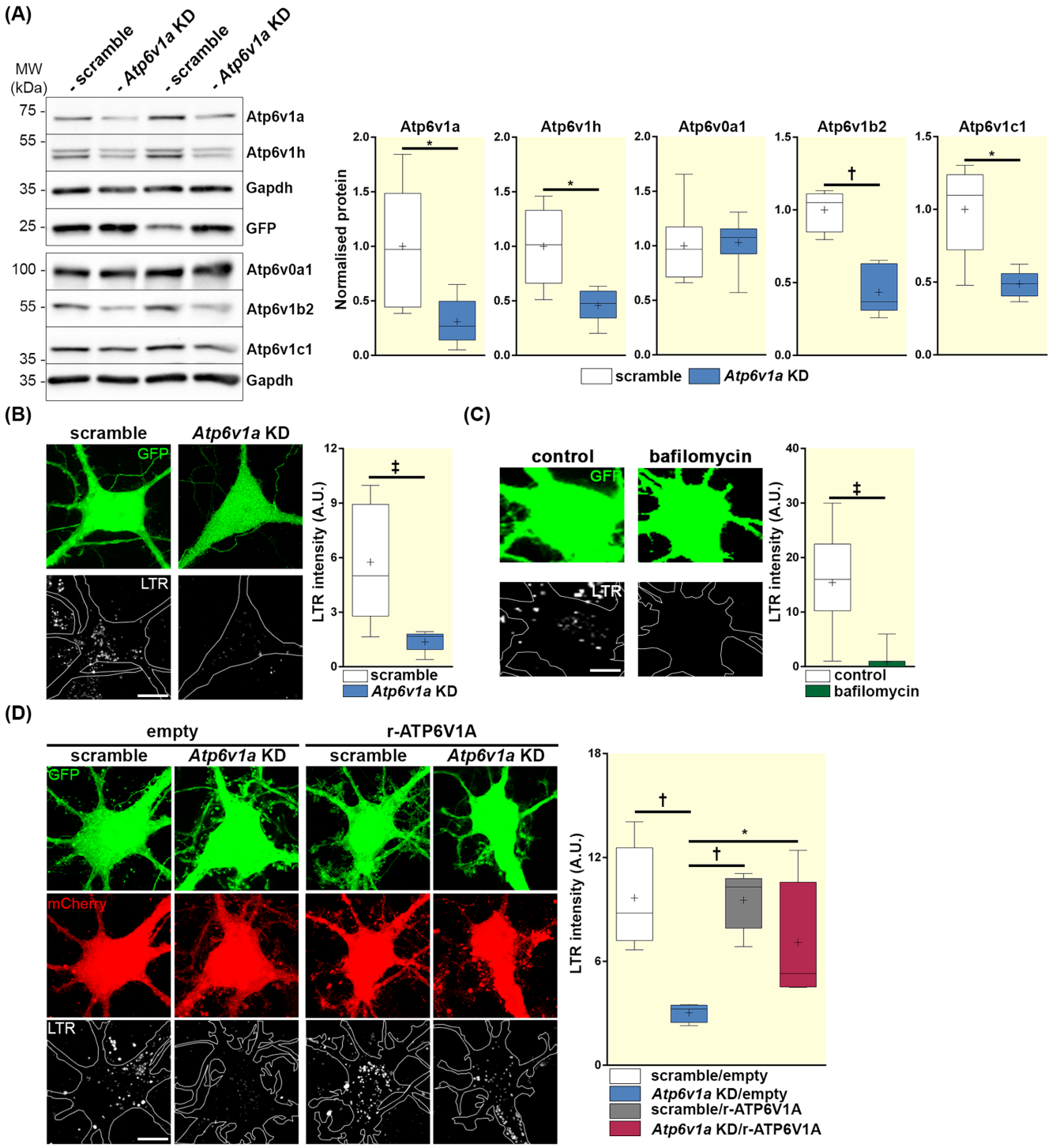

miniature excitatory postsynaptic currents (mEPSCs). We recorded voltage (−70 mV) clamped neurons in the presence of TTX to measure spontaneous miniature currents (Figure 5A). We found that the mEPSC frequency recorded in *Atp6v1a* KD neurons was significantly lower compared to that in controls (scramble: 1.423 Hz ± 0.175; *Atp6v1a* KD: 0.487 Hz ± 0.070; Figure 5B), without significant changes in mEPSC amplitude, charge, rise and decay kinetics (Figure 5C,D). At the ultrastructural level, *Atp6v1a* KD synapses are preserved in term of synaptic area, active zone (AZ) length and total SV density. However, they present accumulation of enlarged cisternae suggesting impaired endosomal clearance at presynaptic sites (Figure 6).

Altogether, these findings suggest a specific loss of active excitatory contacts in *Atp6v1a* silenced neurons with a presynaptic deficit but preserved postsynaptic response to glutamate exocytosis.

17481716, 2024, 8, Downloaded from https://onlinelibrary.wiley.com/doi/10.1111/apha.14186 by Universita Di Firenze Sistema, Wiley Online Library on [04/08/2026]. See the Terms and Conditions (https://onlinelibrary.wiley.com/terms-and-conditions) on Wiley Online Library for rules of use; OA articles are governed by the applicable Creative Commons License

FIGURE 1 Loss of *Atp6v1a* impairs the expression of V1 subunits and acidification of intracellular organelles. (A) Representative Western blot images showing v-ATPase protein levels in rat cortical neuronal transduced with control scramble sh-RNA (scramble) or *Atp6v1a* sh-RNA (*Atp6v1a* KD) pGFP-C-shLenti vectors. Gapdh and turbo-GFP (GFP) are shown as reporters of equal loading and transduction levels. Densitometric quantification is shown on the right. Data are from $n = 6$ independent preparations. *$p < 0.05$, †$p < 0.01$ Mann–Whitney's *U*-test. (B) Representative images of rat hippocampal neurons transduced with scrambled or *Atp6v1a* KD sh-RNAs pGFP-C-shLenti vectors (GFP) and incubated with LysoTracker (LTR, 50 nM, 30 min) at 17 DIV. Quantitative analysis of LTR fluorescence intensity is shown on the right. Data are from 8 to 9 coverslips from 2 independent preparations. ‡$p < 0.001$, unpaired Student's *t*-test. Scale bar 10 μm. (C) Representative images of rat hippocampal neurons transfected with pCAGIG-IRES-enhanced green fluorescent protein (GFP) under control conditions or treated with bafilomycin (100 nM, 3 h) and incubated with LTR as above. Quantitative analysis of LTR fluorescence intensity is shown on the right. Data are from 32 cells for each experimental condition from 3 independent preparations. ‡$p < 0.001$, Mann–Whitney's *U*-test. Scale bar, 5 μm. (D) Representative images of rat hippocampal neurons transduced with scramble or *Atp6v1a* KD sh-RNAs pGFP-C-shLenti vectors (GFP), successively transfected with sh-resistant ATP6V1A in pLVX-IRES-mCherry (r-ATP6V1A) or pLVX-IRES-mCherry empty vector (empty). At 17 DIV neurons were incubated with LTR as above. Quantitative analysis of LTR fluorescence intensity is shown on the right. Data are from 5 coverslips from 2 independent preparations. *$p < 0.05$; †$p < 0.01$, versus *Atp6v1a* KD/empty two-way ANOVA Dunnett's multiple comparison test. Scale bar, 10 μm.

2.6 | *Atp6v1a* silencing impairs autophagy-dependent synaptic plasticity

Compelling evidence demonstrated that lysosomal trafficking and autophagy regulate synaptic activity and plasticity.[30–37] To investigate this aspect, we challenged *Atp6v1a*-silenced neurons with an established chemical long-term potentiation (cLTP) protocol (Figure S4A)[33] and analyzed the excitatory synapses rearrangement. We observed a boost in neuronal autophagy upon LTP induction, as demonstrated by increased Lc3-II and decreased p62 signals, accompanied by the previously reported increase in excitatory synaptic contacts[33] (Figure S4B–F). In contrast, by challenging with the cLTP protocol either *Atp6v1a*-silenced neurons (Figure 7A,B) or bafilomycin-treated neurons (Figure 7C,D), we found that the increase in excitatory synapses was virtually abolished in both experimental groups. These findings demonstrate that neuronal v-ATPase is fundamental for synapse stabilization and plasticity, and loss of V_1 subunit results in defective functional connectivity and plasticity.

3 | DISCUSSION

v-ATPase is a ubiquitously expressed multi-subunit proton pump that regulates several essential functions in cells, ranging from nutrient sensing to catabolism. In neurons, it additionally regulates SV loading and neurotransmission. In recent years, several mutations in genes coding for the various v-ATPase subunits have been described in patients with neurodevelopmental disorders, often associated with epilepsy and intellectual disability. In particular, mutations in *ATP6V1A*, coding for the V_1A member of the cytosolic V_1 complex, have been associated with epileptic encephalopathies and a broad spectrum of clinical severity.[14,16,38–40] Altered ATP6V1A expression has been recently identified in Alzheimer's patient brains and proposed to represent a key factor for neuronal impairment and neurodegeneration.[20] In this scenario, clarifying the morphological and functional consequences of neuronal ATP6V1A loss is fundamental to unravel disease pathophysiology and design novel treatments.

By selectively silencing *Atp6v1a* subunit in rat hippocampal neurons, we observed impairment of lysosomal acidification and of autophagy progression, with an accumulation of aberrant lysosomes and MLB at neuronal soma. This phenotype was accompanied by impaired neuronal arborization and a prominent loss of excitatory synapses. This defect was due to a selective pruning of presynaptic contacts as demonstrated morphologically, by selective decrease of the glutamatergic presynaptic marker and, functionally, by a significant decrease in mEPSCs frequency. At the ultrastructural level, synaptic terminals showed accumulation of enlarged vacuoles with preserved AZ length and SV density within the boutons. The vacuole accumulation may represent a compensatory mechanism that allows the maintenance of the SV pool and their quantal size, as revealed by the preserved amplitude of mEPSCs. A similar, selective loss of presynaptic contacts has been recently described in human neurons lacking ATP6V1A accompanied by impaired neuronal activity.[20] Overall, our results support the evidence for v-ATPase-dependent lysosomal function and autophagy progression that is required for the maintenance of functionally active presynaptic contacts. In neurons lacking Atp6v1a, not only neuronal development and formation of excitatory synaptic connections were defective but also the surviving excitatory synapses did not respond to an LTP protocol that triggered synaptic plasticity in healthy neurons. This defective synaptic plasticity was associated with the lack of autophagy progression, as revealed by the prominent autophagy stimulation upon LTP induction. These data support the emerging and complex role

17481716, 2024, 8, Downloaded from https://onlinelibrary.wiley.com/doi/10.1111/apha.14186 by Universita Di Firenze Sistema, Wiley Online Library on [04/08/2026]. See the Terms and Conditions (https://onlinelibrary.wiley.com/terms-and-conditions) on Wiley Online Library for rules of use; OA articles are governed by the applicable Creative Commons License

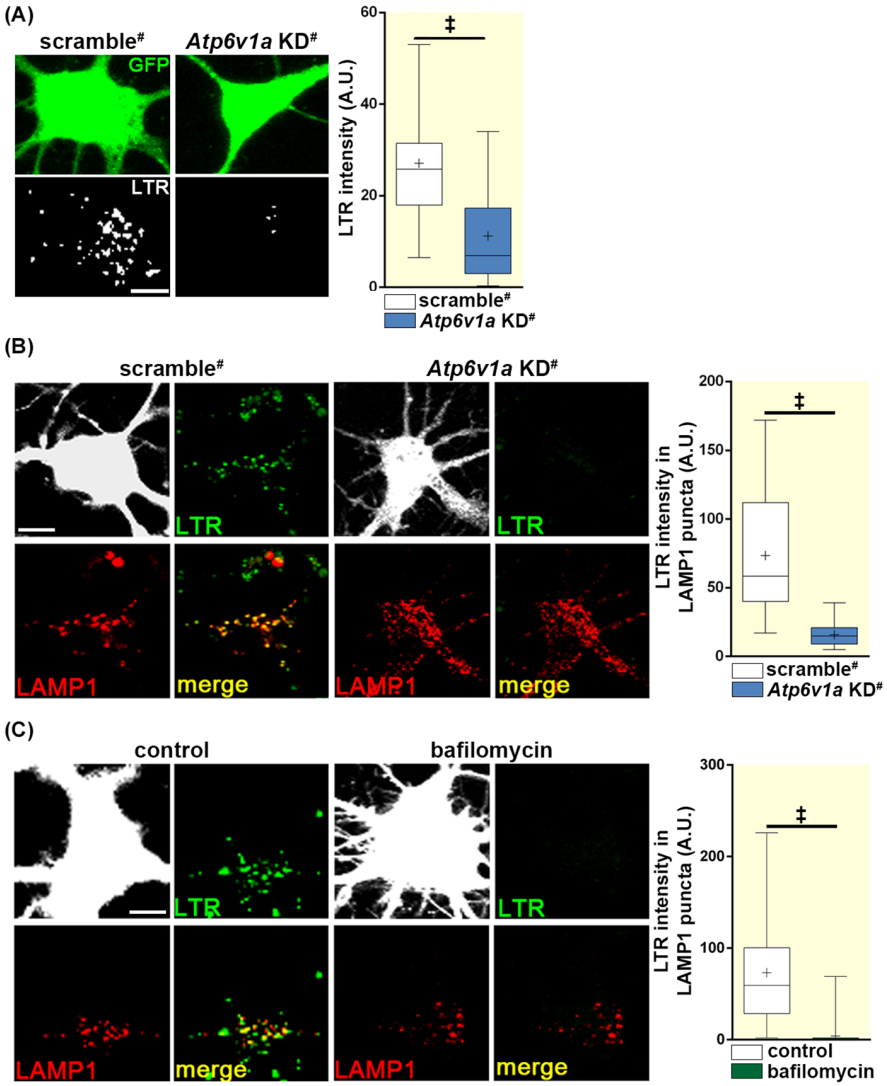

FIGURE 2 The acidic shift in *Atp6v1a* KD neurons primarily involves lysosomes. (A) Representative images of rat hippocampal neurons transfected (#) with scramble or *Atp6v1a* KD sh-RNAs pGFP-C-shLenti vector (GFP) and incubated with LTR (50 nM, 30 min). Quantitative analysis of LTR fluorescence intensity is shown on the right. Data are from 26 scramble and 33 *Atp6v1a* KD neurons from 3 independent preparations. ǂ$p < 0.001$, unpaired Student's *t*-test with Welch's correction. (B) Representative images of rat hippocampal neurons co-transfected with LAMP1-RFP (LAMP1) and either control scramble sh-RNA (scramble) or *Atp6v1a* sh-RNA (*Atp6v1a* KD) pGFP-C-shLenti vector (GFP) and incubated with LTR as above. Quantitative analysis of LTR fluorescence intensity in LAMP1-positive puncta is shown on the right. Data are from 74 scramble and 75 *Atp6v1a* KD neurons from 3 independent preparations. ǂ$p < 0.001$, Mann–Whitney's *U*-test. (C) Representative images of rat hippocampal neurons co-transfected with GFP plasmid (GFP) and LAMP1-RFP (LAMP1) under either control conditions or treated with bafilomycin (100 nM, 3 h). Quantitative analysis of LTR fluorescence intensity in LAMP1-positive puncta is shown on the right. Data are from 66 neurons for each experimental condition obtained from 3 independent preparations. ǂ$p < 0.001$, Mann–Whitney's *U*-test. Scale bars, 10 μm.

of the autophagy process in different forms of synaptic plasticity acting at both presynaptic and postsynaptic compartments.[31,32,36,41,42]

Our findings emphasize the central role of even a single v-ATPase subunit in the regulation of presynaptic homeostasis, synaptic rearrangements and plasticity. The loss of expression of Atp6v1a is paralleled by reduction of its main partners in the cytosolic V_1 domain, whereas no similar decrease is detected for Atp6v0a1, a member of the membrane embedded V_0 domain. These findings are consistent with the reported independent biosynthetic origin of V_0 and V_1 subunits[43] and demonstrate an overall decrease of the cytosolic enzymatic V_1 subunit in *Atp6v1a*-silenced neurons. The closely similar phenotypes which were observed by molecular silencing of *Atp6v1a* and pharmacological v-ATPase inhibition by bafilomycin,

17481716, 2024, 8, Downloaded from https://onlinelibrary.wiley.com/doi/10.1111/apha.14186 by Universita Di Firenze Sistema, Wiley Online Library on [04/08/2026]. See the Terms and Conditions (https://onlinelibrary.wiley.com/terms-and-conditions) on Wiley Online Library for rules of use; OA articles are governed by the applicable Creative Commons License

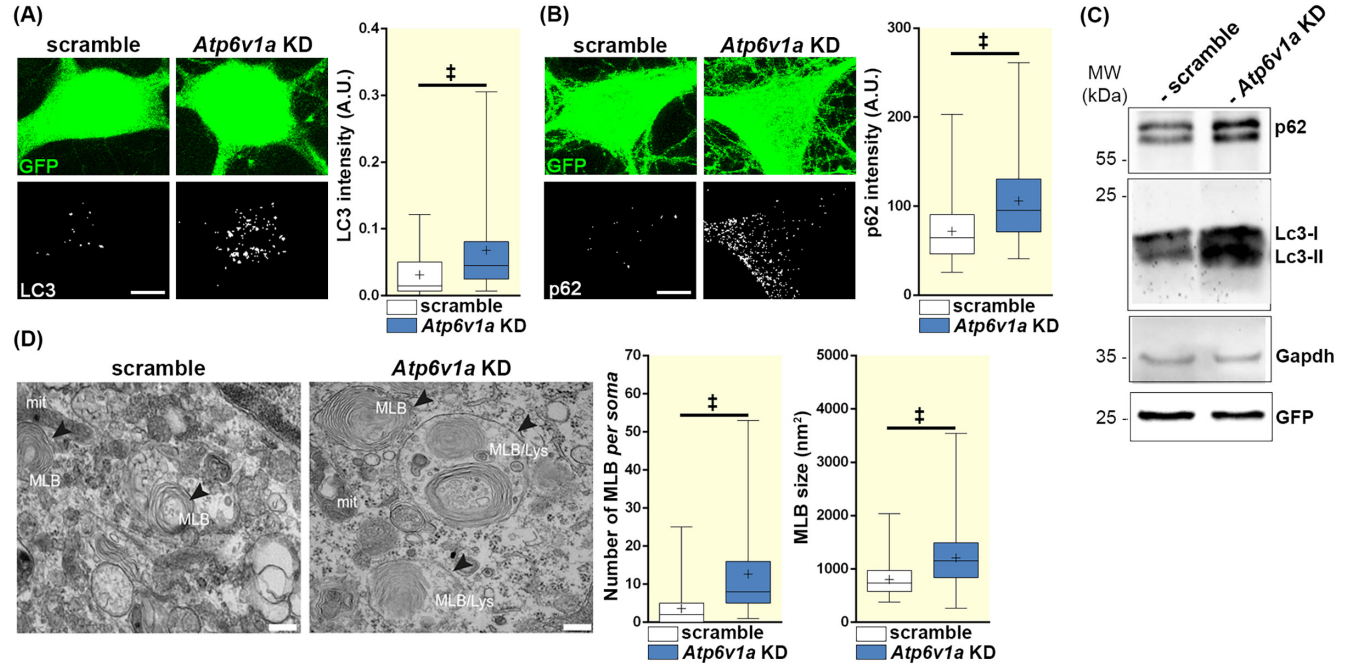

FIGURE 3 *Atp6v1a*-silencing in neurons induces blockade of autophagy and lysosomal structural alterations. (A) Representative images of rat hippocampal neurons transduced with scramble or *Atp6v1a* KD sh-RNAs pGFP-C-shLenti vector (GFP) and successively transfected with LC3-RFP (LC3). Quantitative analysis of LC3-RFP fluorescence intensity is shown on the right. Data are from 39 scramble and 51 *Atp6v1a* KD neurons from 2 independent preparations. ǂ$p < 0.001$, Mann–Whitney's *U*-test. (B) Representative images of rat hippocampal neurons transduced with scramble or *Atp6v1a* KD sh-RNAs pGFP-C-shLenti vector (GFP) and immunostained with anti-p62 antibody. Quantitative analysis of p62 fluorescence intensity is shown on the right. Data are from 50 scramble and 60 *Atp6v1a* KD neurons from 2 independent preparations. ǂ$p < 0.001$, Mann–Whitney's *U*-test. Scale bar, 5 μm. (C) Protein levels of p62, Lc3I and Lc3-II detected by Western blot in transduced neurons. Gapdh and GFP are shown as reporters for equal loading and infection levels. (D) Representative TEM micrographs of neurons transduced as above. Arrowheads indicate multilamellar bodies (MLBs) and enlarged lysosomes containing MLB (MLBs/Lys). Mitochondria (mit) are also shown. Scale bar, 200 nm. Box plots on the left represent numbers and size of MLBs in neuronal soma. All parameters were obtained from 48 cells per each condition from 3 independent preparations. ǂ$p < 0.001$, Wilcoxon's and Mann–Whitney's *U*-tests for MLB number and size, respectively.

further demonstrate the pilot role of V_1 expression for the physiological regulation of v-ATPase activity that propells both lysosomal acidification and autophagy flux.

Our findings reveal that neurons are particularly vulnerable to dysregulation of ATP6V1A, with loss of synaptic stability and plasticity as primary signs of neuronal dysfunction. They also highlight the central role of ATP6V1A in presynaptic homeostasis and activity-dependent rearrangement of synaptic connectivity. Our data further support the role of lysosomal integrity and autophagy flux for morphology and maintenance of connectivity in post-mitotic perennial cells such as neurons,[36,44] and explain the prevalence of brain dysfunction in ATP6V1A related disorders.[14,16] The early synaptic defects described here induced by autophagy-lysosomal dysregulation may trigger a pathophysiological cascade which can possibly result in neuronal shrinkage and neurodegeneration. This progression could underlie the early onset of neurodegeneration associated with the more severe expression of the *ATP6V1A*-related neurodevelopmental disorders[16] as well as the late onset AD associated with ATP6V1A loss.[20,21] Considering the broad spectrum of neurological pathologies related to dysregulation of ATP6V1A and the neuronal effects of its loss describe here in, identifying compounds that selectively act on ATP6V1A becomes a priority. Different ATP6V1A selective drugs are available and could establish a significant therapeutic basis. In particular, the immunosuppressive drug FK506 was reported to selectively bind ATP6V1A and exert neuroprotective effects.[45] The histone deacetylase inhibitor NCH-51 is a selective enhancer of ATP6V1A expression and normalizes neuronal impairment and neurodegeneration caused by ATP6V1A deficits.[20] In addition, the small molecule EN6 interacting with cysteine 277 of ATP6V1A increases v-ATPase activity, lysosomal acidification, and autophagy.[46] On the other hand, Kim et al, observed decreased levels of amyotrophic lateral sclerosis associated protein ataxin-2 upon constitutive downregulation of *ATP6V1A* and lowered ataxin-2 levels in cellular models and in the brains of adult mice after administration of the FDA approved ATP6V1A blocker etidronate.[47] These data, although at odds with previous findings showing pathogenicity

17481716, 2024, 8, Downloaded from https://onlinelibrary.wiley.com/doi/10.1111/apha.14186 by Universita Di Firenze Sistema, Wiley Online Library on [04/08/2026]. See the Terms and Conditions (https://onlinelibrary.wiley.com/terms-and-conditions) on Wiley Online Library for rules of use; OA articles are governed by the applicable Creative Commons License

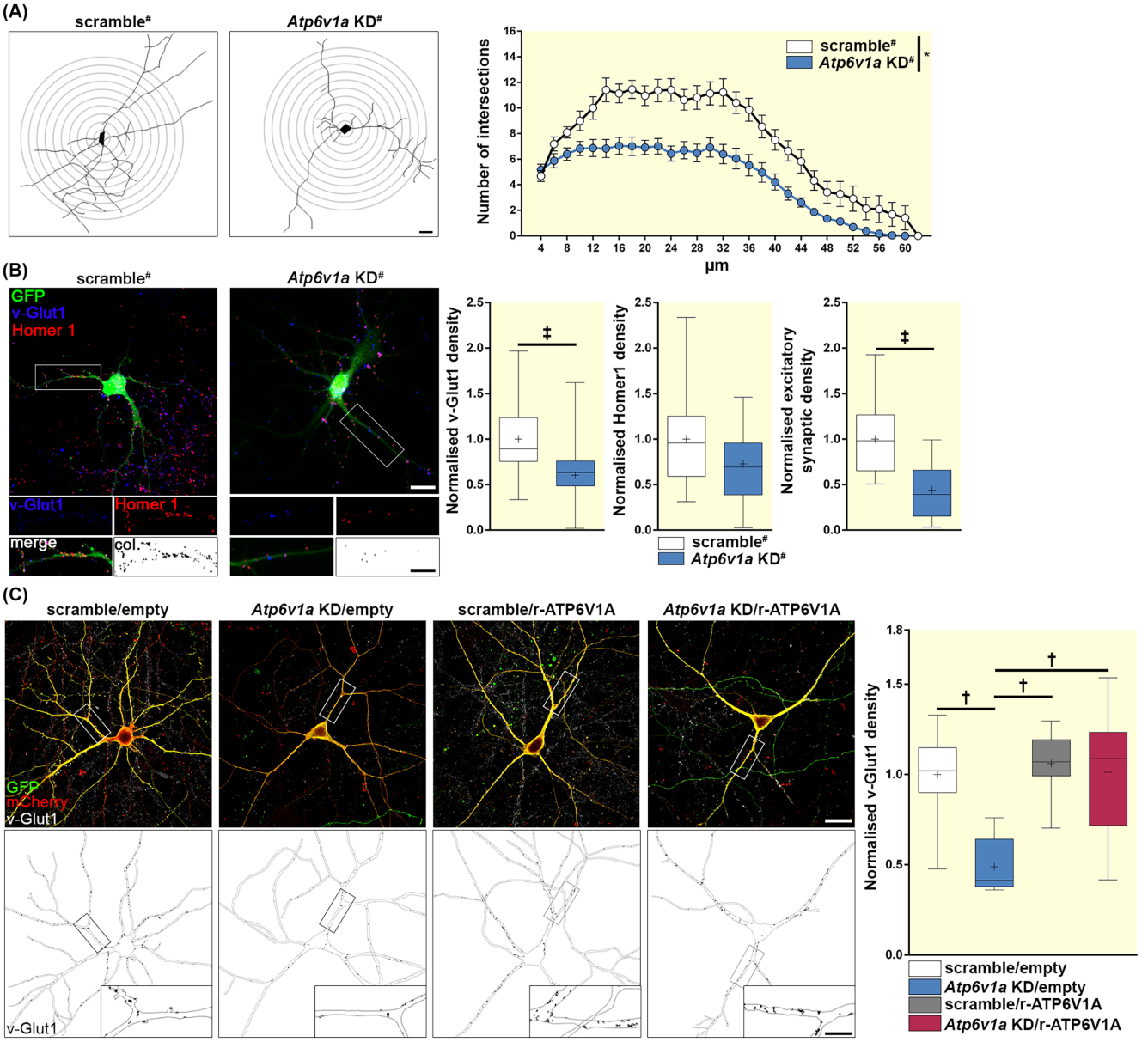

FIGURE 4 *Atp6v1a* silencing impairs dendritic outgrowth and synaptogenesis due to selective loss of presynaptic sites. (A) Representative neuronal reconstructions of rat hippocampal neurons transfected (#) with either control scramble sh-RNA (scramble) or *Atp6v1a* sh-RNA (*Atp6v1a* KD). Concentric circles (one out of three) of increasing radii are superimposed. Sholl analysis of neurite arborization as a function of distance from the soma is shown on the right. Data are mean ± SEM of 17 neurons for each experimental group from 4 independent preparations. *$p < 0.05$, unpaired Student's *t*-test with Welch's correction. Scale bar 10 μm. (B) Representative images of rat hippocampal neurons transfected as in A and double immunostained with v-Glut1 and Homer 1 antibody. White rectangles indicate proximal dendrites shown at higher magnification in the bottom panels. The merge panels show positive puncta along transfected branches. The co-localization panels (col.) highlight the double-positive puncta (black), corresponding to bona fide synapses. Quantitative analysis of double-positive synapses or presynaptic v-Glut1 and postsynaptic Homer 1 single positive puncta counted in the selected regions are shown on the right. Data are from 19 scramble and 22 *Atp6v1a* KD neurons from 3 independent preparations. ‡$p < 0.001$, Mann–Whitney's *U*-test/unpaired Student's *t*-test with Welch's correction. (C) Representative images of rat hippocampal neurons transduced with scramble or *Atp6v1a* KD sh-RNAs pGFP-C-shLenti vector (GFP), successively transfected with sh-resistant ATP6V1A in pLVX-IRES-mCherry (r-ATP6V1A) or pLVX-IRES-mCherry empty vector (empty) and immunostained with v-Glut1 antibody at 17 DIV. Quantitative analysis of v-Glut1 positive puncta counted in the selected regions are shown on the right. Data are from 8 coverslips from each experimental group from 4 independent preparations. †$p < 0.01$, versus *Atp6v1a* KD/empty two-way ANOVA Dunnett's multiple comparison test. Scale bars, 20 μm and 5 μm in higher magnification.

17481716, 2024, 8, Downloaded from https://onlinelibrary.wiley.com/doi/10.1111/apha.14186 by Universita Di Firenze Sistema, Wiley Online Library on [04/08/2026]. See the Terms and Conditions (https://onlinelibrary.wiley.com/terms-and-conditions) on Wiley Online Library for rules of use; OA articles are governed by the applicable Creative Commons License

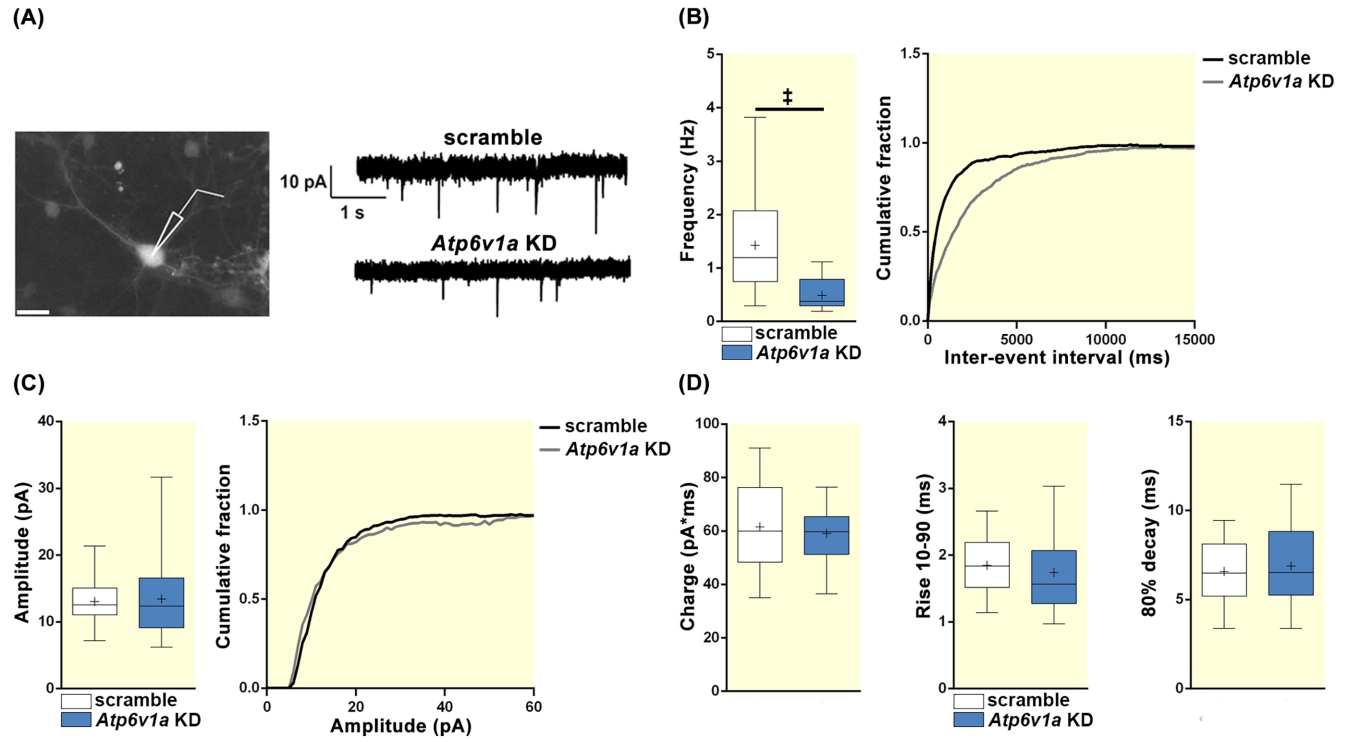

FIGURE 5 Loss of Atp6v1a results in a significant decrease in the frequency of miniature excitatory postsynaptic currents. (A) Representative image (*left*) of primary hippocampal neuron for mEPSC recordings. Scale bar, 20 μm. Representative traces (*right*) of mEPSCs recorded at −70 mV in 17 DIV hippocampal neurons in control and *Atp6v1a* KD neurons. (B) Box plots of the mEPSC frequency (*left*) and cumulative distribution of the inter-event intervals (*right*) in scramble and *Atp6v1a* KD neurons. (C) Box plots of the mEPSC amplitude (*left*) and its cumulative distribution (*right*) in scramble and *Atp6v1a KD* neurons. (D) Box plots representing (*from left to right*) charge, 10–90 rise time and 80% decay time of mEPSCs recorded in scramble and *Atp6v1a KD* neurons. All parameters were obtained from 26 scramble and 15 *Atp6v1a KD* neurons from 3 independent preparations. ǂ$p < 0.001$, Mann–Whitney's *U*-test.

related to decreased ATP6V1A levels,[14,16,19–21] highlight how ATP6V1A levels need to be tightly regulated for neuronal function and survival.

Our data support the pivotal role of ATP6V1A as a target for neurological drug discovery and repositioning and suggest that in *ATP6V1A*-linked diseases acting early on the expression and function of ATP6V1A might preserve synaptic integrity and plasticity to avoid consequent neurodegeneration.

4 | MATERIALS AND METHODS

4.1 | Constructs

Sh-RNA targeting the coding sequence (5′- ACTATGAC AAACACTTCACAGAGTTCGTT-3′) of *Rattus norvegicus Atp6v1a* mRNA (NM_001108318.2; *Atp6v1a KD*) and scramble control cloned into pGFP-C-shLenti Lentiviral vector (#TR30023, Origene) were acquired from Origene. RNAi resistant ATP6V1A isoform, harboring nine silent point mutations into the rat *Atp6v1a* mRNA sequence targeted by sh-RNA (5'-ATTACGATAAGCATTTTACCGAA TTTGTC) cloned into pLVX-IRES-mCherry was acquired from Biomatik. pCAGIG-IRES-enhanced green fluorescent protein (GFP) vector was acquired from Addgene. The production of vesicular stomatitis virus-pseudotyped third-generation lentiviruses was performed as described previously.[48,49] Viral titers ranging from 1.0 to 8.0×10^8 transforming units/mL were obtained. LC3-RFP (#21075) and LAMP1-RFP (#1817) was acquired from Addgene.

4.2 | Primary neuronal and cell cultures preparation, transfection and transduction

Cultures of dissociated primary neurons were prepared from embryonic E18 rats as previously described.[50] Embryonic cortices and hippocampi were dissected and incubated in 0.125% trypsin (Gibco) for 25–30 min at 37°C. Dissociated neurons were plated onto poly-D-lysine-coated coverslips (25 mm) or tissue culture dishes for immunostaining and Western blot, respectively. Primary hippocampal or cortical neurons were infected at 10 DIV with scramble or *Atp6v1a KD*-expressing pGFP-C-shLenti Lentivirus at 10 multiplicity of infection

17481716, 2024, 8, Downloaded from https://onlinelibrary.wiley.com/doi/10.1111/apha.14186 by Universita Di Firenze Sistema, Wiley Online Library on [04/08/2026]. See the Terms and Conditions (https://onlinelibrary.wiley.com/terms-and-conditions) on Wiley Online Library for rules of use; OA articles are governed by the applicable Creative Commons License

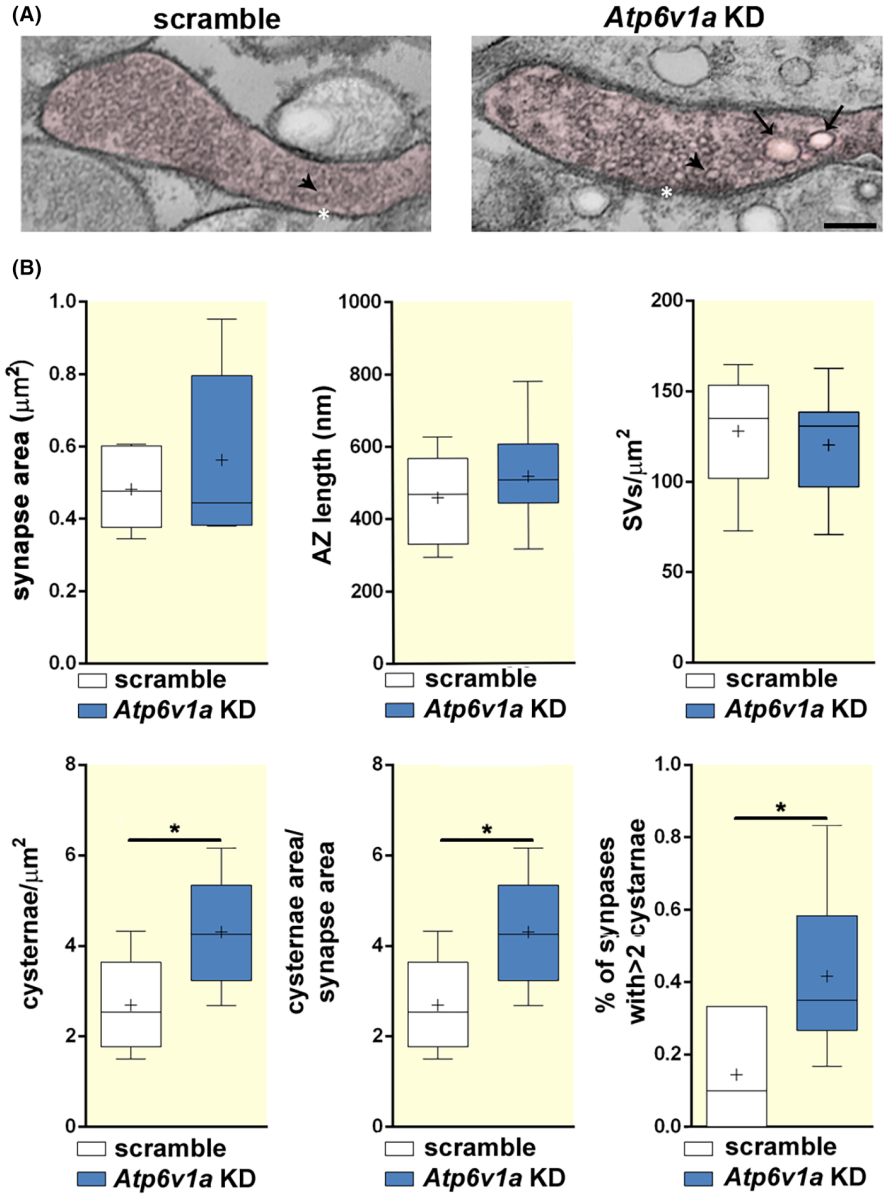

FIGURE 6 Transmission electron microscopy at Atp6v1a deficient synapses. (A) Representative electron micrographs of synaptic terminals from cultured hippocampal neurons transduced with either scramble or the *Atp6v1a* KD sh-RNAs pGFP-C-shLenti vectors. Synaptic area is highlighted in pale pink; * indicates Active Zone (AZ); arrowheads show synaptic vesicles; arrows show cisternae-like structures defined as vesicles larger than 80 nm. Scale bar, 200 nm. (B) Morphometric analysis of the synaptic area, AZ length, SV and cisternae density, synaptic area occupied by cisternae-like structures and number of synapses presenting more than 2 cisternae, under the two experimental conditions. Data are from 6 independent preparations ($n = 45$ and 46 synapses for scramble and Atp6v1a KD, respectively). *$p < 0.05$, Mann–Whitney's U-test or unpaired Student's *t*-test.

(MOI). After 20 h, half of the medium was replaced with fresh medium. When using transfection, neurons were transfected at 14 DIV using Lipofectamine™ 2000 (Thermo Fisher Scientific, #11668019) following manufacturer instruction. All experiments were performed at 17 DIV. When specified neurons were treated 3 h with 100 nM bafilomycin (Tocris Bioscence). For immunocytochemistry experiments, neurons were fixed with 4% paraformaldehyde (PFA, Sigma-Aldrich)/4% sucrose (Applichem) in 1X phosphate-buffered saline (PBS, Sigma-Aldrich) at 37°C for 15 min. HEK293T cells were transiently co-transfected with control scramble sh-RNA or *Atp6v1a* sh-RNAs-pGFP-C-shLenti vector and sh-resistant *ATP6V1A* in pLVX-IRES-mCherry or pLVX-IRES-mCherry empty vector using Lipofectamine™ 2000. 72 h post-transfection cell lysates were collected for Western blot analysis.

4.3 | Western blot analysis

Protein lysates were extracted in lysis buffer (50 mM Tris pH 7.5, 150 mM NaCl, 0.1% SDS, 0.1% Triton™ X-100, 0.2 mM phenylmethylsulphonyl fluoride, 2 μg/mL pepstatin and 1 μg/mL leupeptin), or (100 mM Tris pH 8.0, 10 mM EDTA, 1% SDS). Proteins were quantified by Pierce™ BCA Protein Assay Kits (Thermo Scientific, #23227), loaded and resolved by SDS/PAGE and transferred onto nitrocellulose membranes (Whatman). Membranes were blocked in 1X Tris Buffered Saline (TBS) containing 0.1% Tween-20 and 5% milk for 1 h at room temperature. Then, membranes were incubated at 4°C overnight with the following primary antibodies: anti-LC3B (1:1000; #L7543; Sigma-Aldrich), anti-p62 (1:1000; #P0067; Sigma-Aldrich), anti-GAPDH (1:1000; #SC-25778; Santa Cruz Biotechnology), anti-Atp6v1a antibody (1:1000;

17481716, 2024, 8, Downloaded from https://onlinelibrary.wiley.com/doi/10.1111/apha.14186 by Universita Di Firenze Sistema, Wiley Online Library on [04/08/2026]. See the Terms and Conditions (https://onlinelibrary.wiley.com/terms-and-conditions) on Wiley Online Library for rules of use; OA articles are governed by the applicable Creative Commons License

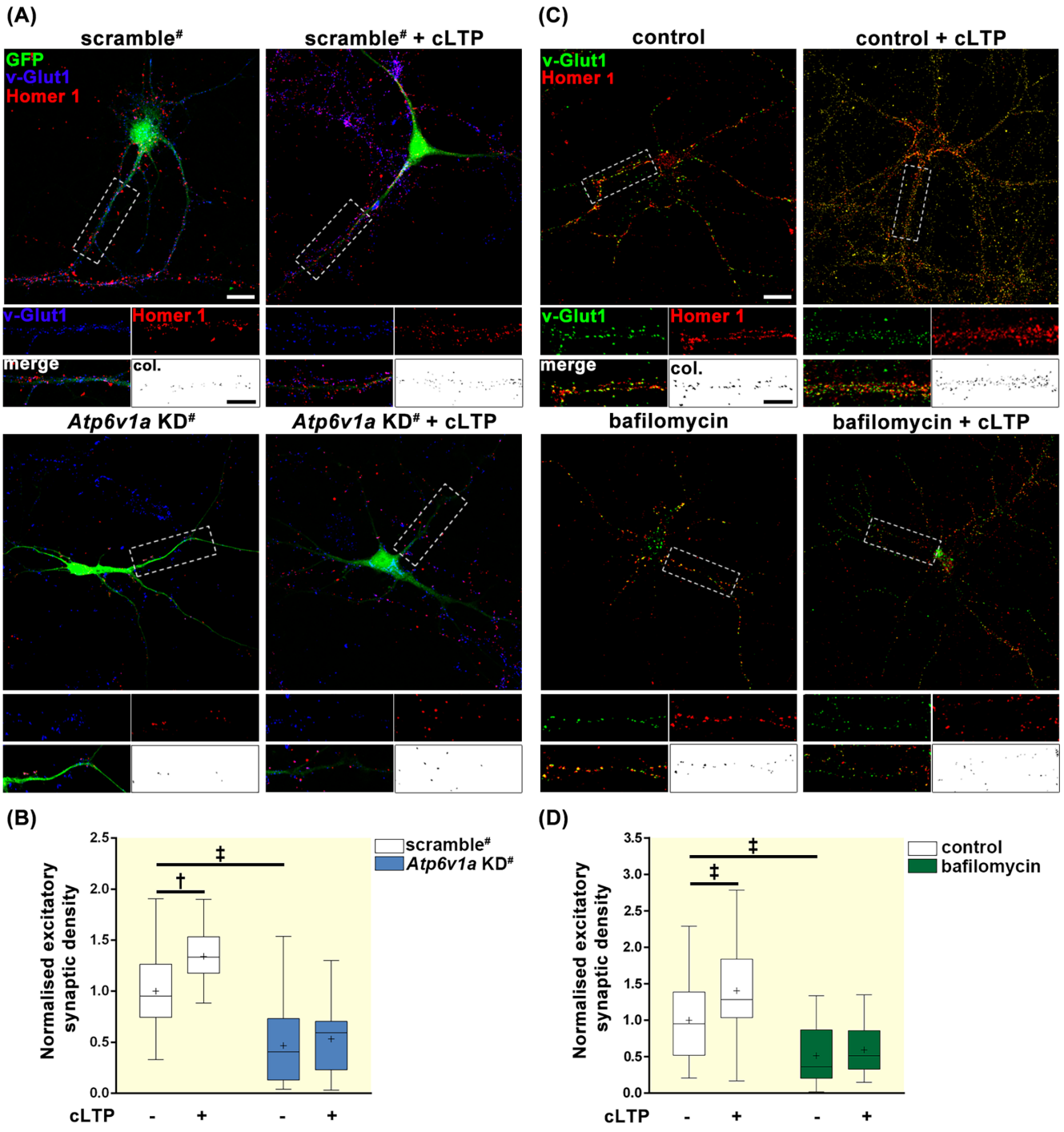

FIGURE 7 *Atp6v1a* silencing impairs autophagy-dependent synaptic plasticity. (A) Representative images of rat hippocampal neurons transfected (#) with either control scramble sh-RNA (scramble) or *Atp6v1a* sh-RNA (*Atp6v1a KD*). Neurons were analyzed under control conditions (*left panels*) or upon stimulation with cLTP (+cLTP, *right panels*). Dashed white rectangles indicate proximal dendrites shown at higher magnification in the bottom panels. Synaptic boutons were identified by double immunostaining for v-Glut1 and Homer 1. The merge panels show positive puncta along transfected branches. The co-localization panels (col.) highlight the double-positive puncta (black), corresponding to bona fide synapses. (B) Quantitative analysis of synaptic puncta counted in the selected regions. Data are from 29 (scramble), 28 (scramble +cLTP), 28 (*Atp6v1a* KD) and 22 (*Atp6v1a* KD + cLTP) neurons from 3 independent preparations. †$p < 0.01$, ‡$p < 0.001$, two-way ANOVA/Tukey's tests. (C) Representative images of rat hippocampal neurons under either control conditions or treated with bafilomycin and exposed to cLTP protocol (+cLTP). Synaptic boutons were identified as in A. (D) Quantitative analysis of synaptic puncta counted in the selected regions. Data are from 48 (control), 61 (control +cLTP), 49 (bafilomycin), and 40 (bafilomycin +cLTP), from 3 independent preparations. ‡$p < 0.001$, two-way ANOVA/Tukey's tests. Scale bars, 20 μm and 5 μm at higher magnification.

17481716, 2024, 8, Downloaded from https://onlinelibrary.wiley.com/doi/10.1111/apha.14186 by Universita Di Firenze Sistema, Wiley Online Library on [04/08/2026]. See the Terms and Conditions (https://onlinelibrary.wiley.com/terms-and-conditions) on Wiley Online Library for rules of use; OA articles are governed by the applicable Creative Commons License

#ab137574; Abcam) and anti-TurboGFP antibody (1:2000; #TA150041; Origene), anti-mCherry antibody (1:1000; # 632543; Clontech), anti-Atp6v1b2 antibody (1:2000; #ab73404; Abcam), anti-Atp6v1h (1:1000; # 26683;), anti-Atp6v1c1 (1:1000; # 16057-1-AP; Proteintech), and anti-ATP6V0a1 antibody (1:1000; #NBP1-89342; Novus). Then, membranes were incubated with HRP-conjugated secondary antibodies and protein bands were revealed with the ECL chemo-luminescence detection system (Thermo Fisher Scientific). Protein signals were acquired using Chemidoc (BioRad).

4.4 | Immunocytochemistry and fluorescence microscopy

Fixed primary hippocampal neurons were permeabilized in 0.1% Triton X-100, incubated 1 h in blocking solution (2% FBS/0.05% TWEEN 20 in 1X PBS) and incubated overnight at 4°C with the following primary antibodies in blocking solution: anti-Atp6v1a antibody (1:400; #ab199326; Abcam), anti-Lc3B (1:200; #2775; Cell Signaling), anti-p62 (1:100; #P0067; Sigma-Aldrich), anti-v-GLUT1 (1:500; #135304; Synaptic Systems), anti-Homer1 (1:200; #160011; Synaptic Systems). Excess antibody was removed by washing coverslips 3 times with 1X PBS and the AlexaFluor-conjugated secondary antibodies (Thermo Fisher Scientific) were added for 1 h. Samples were mounted in ProLong Gold Antifade reagent with DAPI (#P36935, Thermo Fisher Scientific). Capture of confocal images was performed using a laser scanning confocal microscope (SP8, Leica) with a 40x or 63x oil-immersion objective. Each image consisted of a stack of images taken through the z-plane of the cell.

4.5 | LysoTracker experiments

Hippocampal neurons at 17 DIV were incubated with 50 nM LysoTracker Deep Red (#L12492, Thermo Fisher Scientific) for 30 min at 37°C in culture medium and immediately fixed as above. Images were collected within 12 h at the confocal microscope (SP8, Leica). Single confocal plane images were acquired to avoid Lysotracker fluorescent signal fading. Settings were kept the same for all acquisitions within each experiment.

4.6 | Sholl analysis and synapse quantification

For neurite arborization analysis, transfected hippocampal neurons were fixed as above at 17 DIV. The extent of neurite arborization was evaluated using Sholl analysis as previously described.[13] Briefly, concentric circles with radii increasing at regular 4-μm steps were centered to the cell body and the number of intersections was automatically evaluated with the ImageJ/Sholl analysis plug-in.

For synapse quantification, co-localization analysis was performed by evaluating the co-labeling of the v-Glut1/Homer1 synaptic protein couples at 40x. Co-localization puncta with areas of 0.1–2 μm^2 were considered bona fide synaptic boutons. Synaptic boutons along GFP positive neurons were manually counted on cell surface.

4.7 | Electron microscopy

Cells were washed out twice in 0.1 M cacodylate buffer (Sigma-Aldrich, St. Louis, MI, USA) and fixed in 0.1 M cacodylate buffer containing 2.5% glutaraldehyde (Electron Microscopy Science, Hatfield, PA, USA) or 1 h at room temperature. The cells were postfixed in 1% osmium tetroxide for 10 min (VWR International, PA, USA) and 1% aqueous uranyl acetate (SERVA Electrophoresis GmbH, Heidelberg Germany) for 1 h. Subsequently, samples were dehydrated through a graded ethanol series (Merck, Darmstadt, Germany) and flat embedded in epoxy resin (Poly-Bed; Polysciences, Inc., Warrington, PA) for 24 h at 60°C. Ultrathin sections (50 nm) were cut parallel to the substrate and counterstained with 5% uranyl acetate in 50% ethanol. Electron micrographs were acquired using a Hitachi 7800 120Kv electron microscope (Hitachi, Tokyo, Japan) equipped with a Megaview G3 digital camera and Radius software (EMSIS, Muenster, Germany). For EM morphometry on neuronal soma, we classified multilamellar bodies/lysosomes as single-membrane round organelle with electron dense appearance and both onion-like multilamellar and amorphous content. Ten whole cells were scored for lysosomes, counted and measured with line tool of Radius 2.0 software. Morphometric analysis at the synapse was done using NIH ImageJ. Structures with sagittal diameter comprised between 20 and 80 nm were classified as SVs, whereas those with a sagittal diameter bigger than 80 nm were classified as intra-terminal cisternae. Data were analyzed using GraphPad Prism 8 (GraphPad Software, San Diego, CA, USA).

4.8 | Patch-clamp recordings

Whole patch-clamp recordings in voltage-clamp configuration were performed on 17 DIV rat hippocampal primary neurons as previously described.[51,52] Patch pipettes

17481716, 2024, 8, Downloaded from https://onlinelibrary.wiley.com/doi/10.1111/apha.14186 by Universita Di Firenze Sistema, Wiley Online Library on [04/08/2026]. See the Terms and Conditions (https://onlinelibrary.wiley.com/terms-and-conditions) on Wiley Online Library for rules of use; OA articles are governed by the applicable Creative Commons License

were obtained from thin borosilicate glass, pulled to a final resistance of 4–5 MΩ, and filled with internal standard solution. Voltage-clamp recordings for miniature excitatory postsynaptic currents (mEPSCs) were performed at −70 mV holding potential and the recordings were acquired at 10 kHz and filtered at 2 kHz. All experiments were performed at room temperature (22–25°C). Data acquisition was performed using Multiclamp 700B and Clampex program (Axon Elektronic). For mEPSC recordings bicuculline methiodide (30 μM), CGP58845 (5 μM), D-(−)-2-amino-5-phosphonopentanoic acid (D-AP5; 50 μM) and tetrodotoxin (TTX; 300 nM) were added to the extracellular solution to block $GABA_A$, $GABA_B$, NMDA receptors and generation and propagation of spontaneous action potentials (APs). The internal solution (K-gluconate) used for the recording of mEPSCs was composed of (in mM): 126 K gluconate, 4 NaCl, 1 $MgSO_4$, 0.02 $CaCl_2$, 0.1 BAPTA, 15 glucose, 5 Hepes, 3 ATP, and 0.1 GTP (pH 7.3 with KOH). The amplitude and frequency of excitatory miniature events were calculated using a peak detector function using appropriate threshold amplitude and area. The frequency, amplitude and kinetics of mEPSCs were analyzed using the MiniAnalysis (RRID:SCR_002184) and the Prism software (GraphPad Software, Inc.). All reagents were bought by Tocris, otherwise specified in detail.

4.9 | Chemical LTP

To induce synaptic plasticity in cultured primary neurons, we used the glycine-induced synaptic potentiation (GISP) paradigm.[33,53,54] Prior to be exposed to GISP, +cultures were incubated for 30 min in the extracellular control solution (in mM): 125 NaCl, 2.5 KCl, 1 $MgCl_2$, 2 $CaCl_2$, 33 D-glucose, 0.02 D-AP5 (#0106, Tocris), 0.003 strychnine (#S0532, Sigma-Aldrich), 0.02 bicuculline (#2503, Tocris), 0.0005 TTX (#1069, Tocris), and 25 HEPES, pH 7.3. GISP was induced by treating cultures for 17 min adding 200 μM glycine coupled with TTX, Mg^{2+} and D-AP5 removal. After glycine treatment, cultures were incubated with control solution and analyzed 3 h later by Western blot and immunocytochemistry.

4.10 | Statistical analysis

Data are expressed as box plots (center line, median [Q2]; box limits, 25th [Q1]-75th [Q3] percentiles; whisker length, the outermost data points within 3-fold the interquartile range [Q3-Q1]) or mean ± SEM. Normal distribution of data was assessed using the D'Agostino-Pearson's normality test. Data with normal distribution were analyzed by the unpaired Student's t-test with the Welch's correction; non-normally distributed data were analyzed by the Mann–Whitney's *U*-test or the Wilconxon test. Statistical significance between more than two normally distributed groups was evaluated using two-way repeated measures ANOVA with the Tukey's *post hoc* multiple comparisons test. Significance level was preset to $p < 0.05$. Statistical analysis was carried out using Prism (GraphPad Software, Inc., La Jolla, CA).

5 | CONCLUSION

The cytosolic v-ATPase subunit ATP6V1A is a key player for lysosomal function and autophagy in neurons and regulates functional development of synaptic connectivity and plasticity.

AUTHOR CONTRIBUTIONS

Alessandro Esposito: Investigation; formal analysis. **Sara Pepe:** Investigation; formal analysis; visualization. **Maria Sabina Cerullo:** Investigation. **Katia Cortese:** Investigation. **Hanako Tsushima Semini:** Investigation; validation. **Silvia Giovedì:** Investigation. **Renzo Guerrini:** Supervision. **Fabio Benfenati:** Supervision. **Antonio Falace:** Writing – original draft; writing – review and editing; formal analysis; validation; investigation; visualization; methodology. **Anna Fassio:** Conceptualization; funding acquisition; writing – original draft; writing – review and editing; supervision; project administration; formal analysis.

ACKNOWLEDGMENTS

The work of AFas, HTS and SG was supported by #NEXTGENERATIONEU (NGEU) and funded by the Ministry of University and Research (MUR), National Recovery and Resilience Plan (NRRP), project MNESYS (PE0000006)—A multiscale integrated approach to the study of the nervous system in health and disease (DN. 1553 11.10.2022). SP was suppoted by the Italian Ministry of Health (Ricerca Finalizzata Giovani Ricercatori GR-2019-12 370 176). RG was supported by the Tuscany Region Call for Health 2018 (grant DECODE-EE) and Fondazione Cassa di Risparmio di Firenze (Human Brain Optical Mapping Project) . We also thank IRCCS Ospedale Policlinico San Martino (5x1000 and Ricerca Corrente), the University of Genoa for funding the acquisition of the HITACHI 120 kV TEM microscope HT7800 (Grant D.R. 3404, Heavy Equipment) and SIlvia Casagrande and Maria Cristina Gagliani for technical assistance . Open access funding provided by BIBLIOSAN.

CONFLICT OF INTEREST STATEMENT

The authors declare no competing financial interests.

17481716, 2024, 8, Downloaded from https://onlinelibrary.wiley.com/doi/10.1111/apha.14186 by Universita Di Firenze Sistema, Wiley Online Library on [04/08/2026]. See the Terms and Conditions (https://onlinelibrary.wiley.com/terms-and-conditions) on Wiley Online Library for rules of use; OA articles are governed by the applicable Creative Commons License

DATA AVAILABILITY STATEMENT

The data that support the findings of this study are available from the corresponding author upon reasonable request.

ORCID

Sara Pepe https://orcid.org/0009-0000-0357-2651
Fabio Benfenati https://orcid.org/0000-0002-0653-8368
Anna Fassio https://orcid.org/0000-0002-8801-038X

REFERENCES

1. Forgac M. Vacuolar ATPases: rotary proton pumps in physiology and pathophysiology. *Nat Rev Mol Cell Biol*. 2007;8(11):917-929. doi:10.1038/nrm2272
2. McGuire CM, Forgac M. Glucose starvation increases V-ATPase assembly and activity in mammalian cells through AMP kinase and phosphatidylinositide 3-kinase/Akt signaling. *J Biol Chem*. 2018;293(23):9113-9123. doi:10.1074/jbc.RA117.001327
3. Ratto E, Chowdhury SR, Siefert NS, et al. Direct control of lysosomal catabolic activity by mTORC1 through regulation of V-ATPase assembly. *Nat Commun*. 2022;13(1):4848. doi:10.1038/s41467-022-32515-6
4. Stransky L, Cotter K, Forgac M. The function of V-ATPases in cancer. *Physiol Rev*. 2016;96(3):1071-1091. doi:10.1152/physrev.00035.2015
5. Smith GA, Howell GJ, Phillips C, Muench SP, Ponnambalam S, Harrison MA. Extracellular and luminal pH regulation by vacuolar H+-ATPase isoform expression and targeting to the plasma membrane and endosomes. *J Biol Chem*. 2016;291(16):8500-8515. doi:10.1074/jbc.M116.723395
6. Toei M, Saum R, Forgac M. Regulation and isoform function of the V-ATPases. *Biochemistry*. 2010;49(23):4715-4723. doi:10.1021/bi100397s
7. Stavoe AKH, Holzbaur ELF. Autophagy in neurons. *Annu Rev Cell Dev Biol*. 2019;35:477-500. doi:10.1146/annurev-cellbio-100818-125242
8. Gowrisankaran S, Milosevic I. Regulation of synaptic vesicle acidification at the neuronal synapse. *IUBMB Life*. 2020;72(4):568-576. doi:10.1002/iub.2235
9. Takamori S, Holt M, Stenius K, Lemke EA, Gronborg M, et al. Molecular anatomy of a trafficking organelle. *Cell*. 2006;127(4):831-846. doi:10.1016/j.cell.2006.10.030
10. Aoto K, Kato M, Akita T, et al. ATP6V0A1 encoding the a1-subunit of the V0 domain of vacuolar H(+)-ATPases is essential for brain development in humans and mice. *Nat Commun*. 2021;12(1):2107. doi:10.1038/s41467-021-22389-5
11. Beauregard-Lacroix E, Pacheco-Cuellar G, Ajeawung NF, et al. DOORS syndrome and a recurrent truncating ATP6V1B2 variant. *Genet Med*. 2021;23(1):149-154. doi:10.1038/s41436-020-00950-9
12. Bott LC, Forouhan M, Lieto M, et al. Variants in ATP6V0A1 cause progressive myoclonus epilepsy and developmental and epileptic encephalopathy. *Brain Commun*. 2021;3(4):fcab245. doi:10.1093/braincomms/fcab245
13. Esposito A, Falace A, Wagner M, et al. Biallelic DMXL2 mutations impair autophagy and cause Ohtahara syndrome with progressive course. *Brain*. 2019;142(12):3876-3891. doi:10.1093/brain/awz326
14. Fassio A, Esposito A, Kato M, et al. De novo mutations of the ATP6V1A gene cause developmental encephalopathy with epilepsy. *Brain*. 2018;141(6):1703-1718. doi:10.1093/brain/awy092
15. Fassio A, Falace A, Esposito A, Aprile D, Guerrini R, Benfenati F. Emerging role of the autophagy/lysosomal degradative pathway in neurodevelopmental disorders with epilepsy. *Front Cell Neurosci*. 2020;14:39. doi:10.3389/fncel.2020.00039
16. Guerrini R, Mei D, Kerti-Szigeti K, et al. Phenotypic and genetic spectrum of ATP6V1A encephalopathy: a disorder of lysosomal homeostasis. *Brain*. 2022;145(8):2687-2703. doi:10.1093/brain/awac145
17. Hirose T, Cabrera-Socorro A, Chitayat D, Lemonnier T, Feraud O, et al. ATP6AP2 variant impairs CNS development and neuronal survival to cause fulminant neurodegeneration. *J Clin Invest*. 2019;129(5):2145-2162. doi:10.1172/JCI79990
18. Zhao W, Gao X, Qiu S, et al. A subunit of V-ATPases, ATP6V1B2, underlies the pathology of intellectual disability. *EBioMedicine*. 2019;45:408-421. doi:10.1016/j.ebiom.2019.06.035
19. Neff RA, Wang M, Vatansever S, et al. Molecular subtyping of Alzheimer's disease using RNA sequencing data reveals novel mechanisms and targets. *Sci Adv*. 2021;7:2. doi:10.1126/sciadv.abb5398
20. Wang M, Li A, Sekiya M, et al. Transformative network modeling of multi-omics data reveals detailed circuits, key regulators, and potential therapeutics for Alzheimer's disease. *Neuron*. 2021;109:257-272.e14. doi:10.1016/j.neuron.2020.11.002
21. Zhou Z, Bai J, Zhong S, et al. Downregulation of ATP6V1A involved in Alzheimer's disease via synaptic vesicle cycle, phagosome, and oxidative phosphorylation. *Oxidative Med Cell Longev*. 2021;2021:5555634. doi:10.1155/2021/5555634
22. Abbas YM, Wu D, Bueler SA, Robinson CV, Rubinstein JL. Structure of V-ATPase from the mammalian brain. *Science*. 2020;367(6483):1240-1246. doi:10.1126/science.aaz2924
23. Di Giovanni J, Boudkkazi S, Mochida S, Bialowas A, Samari N, et al. V-ATPase membrane sector associates with synaptobrevin to modulate neurotransmitter release. *Neuron*. 2010;67(2):268-279. doi:10.1016/j.neuron.2010.06.024
24. Leveque C, Maulet Y, Wang Q, Rame M, Rodriguez L, et al. A role for the V0 sector of the V-ATPase in Neuroexocytosis: exogenous V0d blocks complexin and SNARE interactions with V0c. *Cells*. 2023;12:5. doi:10.3390/cells12050750
25. Bodzeta A, Kahms M, Klingauf J. The presynaptic v-ATPase reversibly disassembles and thereby modulates exocytosis but is not part of the fusion machinery. *Cell Rep*. 2017;20(6):1348-1359. doi:10.1016/j.celrep.2017.07.040
26. Farsi Z, Gowrisankaran S, Krunic M, et al. Clathrin coat controls synaptic vesicle acidification by blocking vacuolar ATPase activity. *elife*. 2018;7:e32569. doi:10.7554/eLife.32569
27. Colacurcio DJ, Nixon RA. Disorders of lysosomal acidification-the emerging role of v-ATPase in aging and neurodegenerative disease. *Ageing Res Rev*. 2016;32:75-88. doi:10.1016/j.arr.2016.05.004
28. Qiu S, Zhao W, Gao X, et al. Syndromic deafness gene ATP6V1B2 controls degeneration of spiral ganglion neurons through modulating proton flux. *Front Cell Dev Biol*. 2021;9:742714. doi:10.3389/fcell.2021.742714
29. Wu JJ, Cai A, Greenslade JE, et al. ALS/FTD mutations in UBQLN2 impede autophagy by reducing autophagosome acidification through loss of function. *Proc Natl Acad Sci USA*. 2020;117(26):15230-15241. doi:10.1073/pnas.1917371117

17481716, 2024, 8, Downloaded from https://onlinelibrary.wiley.com/doi/10.1111/apha.14186 by Universita Di Firenze Sistema, Wiley Online Library on [04/08/2026]. See the Terms and Conditions (https://onlinelibrary.wiley.com/terms-and-conditions) on Wiley Online Library for rules of use; OA articles are governed by the applicable Creative Commons License

30. Cheng A, Tse KH, Chow HM, et al. ATM loss disrupts the autophagy-lysosomal pathway. *Autophagy*. 2021;17(8):1998-2010. doi:10.1080/15548627.2020.1805860
31. Compans B, Camus C, Kallergi E, et al. NMDAR-dependent long-term depression is associated with increased short term plasticity through autophagy mediated loss of PSD-95. *Nat Commun*. 2021;12(1):2849. doi:10.1038/s41467-021-23133-9
32. Daskalaki AD, Kallergi E, Kolaxi A, Nikoletopoulou V. Local biogenesis of autophagic vesicles in neuronal dendrites facilitates long-term synaptic depression. *Autophagy*. 2022;18(8):2011-2012. doi:10.1080/15548627.2022.2061757
33. Glatigny M, Moriceau S, Rivagorda M, et al. Autophagy is required for memory formation and reverses age-related memory decline. *Curr Biol*. 2019;29(3):435-448.e8. doi:10.1016/j.cub.2018.12.021
34. Goo MS, Sancho L, Slepak N, et al. Activity-dependent trafficking of lysosomes in dendrites and dendritic spines. *J Cell Biol*. 2017;216(8):2499-2513. doi:10.1083/jcb.201704068
35. Hoffmann S, Orlando M, Andrzejak E, et al. Light-activated ROS production induces synaptic autophagy. *J Neurosci*. 2019;39(12):2163-2183. doi:10.1523/JNEUROSCI.1317-18.2019
36. Overhoff M, Tellkamp F, Hess S, et al. Autophagy regulates neuronal excitability by controlling cAMP/protein kinase a signaling at the synapse. *EMBO J*. 2022;41(22):e110963. doi:10.15252/embj.2022110963
37. Yang S, Park D, Manning L, et al. Presynaptic autophagy is coupled to the synaptic vesicle cycle via ATG-9. *Neuron*. 2022;110:824-840.e10. doi:10.1016/j.neuron.2021.12.031
38. Li B, Lan S, Liu XR, et al. ATP6V1A variants are associated with childhood epilepsy with favorable outcome. *Seizure*. 2023;116:81-86. doi:10.1016/j.seizure.2023.08.004
39. Van Damme T, Gardeitchik T, Mohamed M, Guerrero-Castillo S, Freisinger P, et al. Mutations in ATP6V1E1 or ATP6V1A cause autosomal-recessive cutis Laxa. *Am J Hum Genet*. 2017;100(2):216-227. doi:10.1016/j.ajhg.2016.12.010
40. Vogt G, El Choubassi N, Herczegfalvi A, Kolbel H, Lekaj A, et al. Expanding the clinical and molecular spectrum of ATP6V1A related metabolic cutis laxa. *J Inherit Metab Dis*. 2021;44(4):972-986. doi:10.1002/jimd.12341
41. Gundelfinger ED, Karpova A, Pielot R, Garner CC, Kreutz MR. Organization of presynaptic autophagy-related processes. *Front Synaptic Neurosci*. 2022;14:829354. doi:10.3389/fnsyn.2022.829354
42. Xuan Z, Yang S, Clark B, Hill SE, Manning L, Colón-Ramos DA. The active zone protein clarinet regulates synaptic sorting of ATG-9 and presynaptic autophagy. *PLoS Biol*. 2023;21(4):e3002030. doi:10.1371/journal.pbio.3002030
43. Wang H, Bueler SA, Rubinstein JL. Structural basis of V-ATPase V(O) region assembly by Vma12p, 21p, and 22p. *Proc Natl Acad Sci USA*. 2023;120(6):e2217181120. doi:10.1073/pnas.2217181120
44. Nikoletopoulou V, Papandreou ME, Tavernarakis N. Autophagy in the physiology and pathology of the central nervous system. *Cell Death Differ*. 2015;22(3):398-407. doi:10.1038/cdd.2014.204
45. Kim D, Hwang HY, Kim JY, et al. FK506, an immunosuppressive drug, induces autophagy by binding to the V-ATPase catalytic subunit a in neuronal cells. *J Proteome Res*. 2017;16(1):55-64. doi:10.1021/acs.jproteome.6b00638
46. Chung CY, Shin HR, Berdan CA, Ford B, Ward CC, et al. Covalent targeting of the vacuolar H(+)-ATPase activates autophagy via mTORC1 inhibition. *Nat Chem Biol*. 2019;15(8):776-785. doi:10.1038/s41589-019-0308-4
47. Kim G, Nakayama L, Blum JA, et al. Genome-wide CRISPR screen reveals v-ATPase as a drug target to lower levels of ALS protein ataxin-2. *Cell Rep*. 2022;41(4):111508. doi:10.1016/j.celrep.2022.111508
48. De Palma M, Naldini L. Transduction of a gene expression cassette using advanced generation lentiviral vectors. *Methods Enzymol*. 2002;346:514-529. doi:10.1016/s0076-6879(02)46074-0
49. Verstegen AM, Tagliatti E, Lignani G, Marte A, Stolero T, et al. Phosphorylation of synapsin I by cyclin-dependent kinase-5 sets the ratio between the resting and recycling pools of synaptic vesicles at hippocampal synapses. *J Neurosci*. 2014;34(21):7266-7280. doi:10.1523/JNEUROSCI.3973-13.2014
50. Tagliatti E, Fadda M, Falace A, Benfenati F, Fassio A. Arf6 regulates the cycling and the readily releasable pool of synaptic vesicles at hippocampal synapse. *elife*. 2016;5:e10116. doi:10.7554/eLife.10116
51. Baldelli P, Fassio A, Valtorta F, Benfenati F. Lack of synapsin I reduces the readily releasable pool of synaptic vesicles at central inhibitory synapses. *J Neurosci*. 2007;27(49):13520-13531. doi:10.1523/JNEUROSCI.3151-07.2007
52. Chiappalone M, Casagrande S, Tedesco M, et al. Opposite changes in glutamatergic and GABAergic transmission underlie the diffuse hyperexcitability of synapsin I-deficient cortical networks. *Cereb Cortex*. 2009;19(6):1422-1439. doi:10.1093/cercor/bhn182
53. Lu W, Man H, Ju W, Trimble WS, MacDonald JF, et al. Activation of synaptic NMDA receptors induces membrane insertion of new AMPA receptors and LTP in cultured hippocampal neurons. *Neuron*. 2001;29(1):243-254. doi:10.1016/s0896-6273(01)00194-5
54. Oh MC, Derkach VA. Dominant role of the GluR2 subunit in regulation of AMPA receptors by CaMKII. *Nat Neurosci*. 2005;8(7):853-854. doi:10.1038/nn1476

SUPPORTING INFORMATION

Additional supporting information can be found online in the Supporting Information section at the end of this article.

How to cite this article: Esposito A, Pepe S, Cerullo MS, et al. ATP6V1A is required for synaptic rearrangements and plasticity in murine hippocampal neurons. *Acta Physiol*. 2024;240:e14186. doi:10.1111/apha.14186

17481716, 2024, 8, Downloaded from https://onlinelibrary.wiley.com/doi/10.1111/apha.14186 by Universita Di Firenze Sistema, Wiley Online Library on [04/08/2026]. See the Terms and Conditions (https://onlinelibrary.wiley.com/terms-and-conditions) on Wiley Online Library for rules of use; OA articles are governed by the applicable Creative Commons License